Theoretical Analysis of Amperometric Biosensor with Substrate and Product Inhibition Involving non - Michaelis - Menten Kinetics

Mallikarjuna M[1], Juan L. G. Guirao[2] and Senthamarai R[1*]

[1]Department of Mathematics, Collage of Engineering and Technology, SRM Institute of Science and Technology, Kattankulathur, 603203, Tamil Nadu, India.
[2]Department of Applied Mathematics and Statistics, Technical University of Cartagena, Hospital de Marina, Cartagena, 30203, Spain.

*Corresponding author(s). E-mail(s): senthamr@srmist.edu.in;

Abstract

In this paper, a non-steady-state amperometric biosensor with the mixed enzyme kinetics and diffusion limitations under the inhibitions of substrate and product is modeled mathematically. The non-steady-state reaction-diffusion equations of the system consist non-linear terms related to an enzymatic reaction of non-Michaelis-Menten kinetics. We have presented the approximate analytical solutions for the concentrations of substrate and product in non-steady and steady-state models using the new approach of Homotopy perturbation method (HPM). The provided expression is presented for all potential diffusion and kinetic parameter values. Analytical expressions of the biosensor current and sensitivity are also presented and discussed. In addition, we also provided numerical solutions for the proposed model by utilizing the pdepe tool in MATLAB software. When comparing the analytical solution with the numerical solution, a satisfactory result is noted for all the possible values of the parameters. Furthermore, the influence of diffusion and kinetic parameters on both the current and the sensitivity are discussed. Analytical expressions for the limiting cases of biosensor enzyme kinetics are presented in this

research article. Additionally, an analytical expression for determining the effective thickness of the membrane is derived and presented.

Keywords: Homotopy perturbation method (HPM), Non-Michaelis–Menten reaction, Amperometric biosensor, Substrate and product inhibition

1 Introduction

Biosensors are analytical devices that detect and measure the concentration of biological or chemical compounds in a sample using a biological recognition element, such as an enzyme. Among the various types of biosensors, amperometric biosensors are particularly attractive due to their high sensitivity, rapid response, and simple operation.Amperometric biosensors detect variations in the electric current produced at the electrode due to the direct oxidation or reduction of a biochemical reaction. An amperometric biosensor typically consists of an electrode, a biological recognition element immobilized on the electrode surface, and a transducer that converts the biochemical signal into an electrical signal [1]-[2]. These biosensors have been widely used in various applications, such as clinical diagnosis, environmental monitoring, and food analysis. They offer advantages over traditional analytical methods, such as high sensitivity, real-time monitoring, and low sample consumption [3]-[5].

Amperometric techniques exhibit a linear relationship between the measured current and analyte concentration in the buffer solution, delivering a current response that increases in direct correlation with rising concentrations, typically within a standard dynamic range. In spite of potential errors in current measurements that may arise as a result of multitude of influencing factors, meticulous calibration and vigilant control of experimental variables guarantee the reliability and precision of these methods for quantifying analyte concentration [6]-[7]. Various models have been developed for biosensors that account for substrate and product inhibition under steady-state [8]-[9] and non-steady-state conditions [10]. To optimize the amperometric biosensor by reducing the substrate and product inhibition in enzyme activity Šimelevičius and Baronas [11] proposed a mathematical model of biosensor considering the mixed enzyme kinetics with both substrate and product inhibition.

Meena and Rajendran [12] utilized the Homotopy perturbation method, which was proposed by Ji Huan He [13] to obtain approximate analytical expressions for concentrations of substrate and product of the non-steady-state reaction-diffusion equations of amperometric biosensor that describe the diffusion coupled with a Michaelis–Menten kinetics and analytical expression of biosensor current are also provided. In the case of substrate inhibition kinetics in enzymatic reaction of amperometric biosensor, Manimozhi et al. [14] derived an analytical expression for the steady-state substrate concentration of the amperometric biosensor with substrate inhibition through the use of the variational iteration method (VIM) and HPM which is proved to the suitable for

all values of parameters. Whereas for the case of the amperometric biosensor's non-steady-state reaction-diffusion equation with substrate inhibition kinetics, an approximate analytical solution for both the substrate concentration and the dimensionless current response was presented in the study by Senthamarai and Jana Ranjani [15]. They employed the Homotopy Perturbation Method (HPM) to derive these solutions.

Swaminathan et al. [16] derived approximate analytical solutions for substrate and product concentrations, current, sensitivity, and resistance in steady-state amperometric biosensors featuring substrate inhibition kinetics, employing both the Taylors series method and the new Homotopy perturbation method. For the product inhibition kinetics, Rani et al. [17] provided mathematical analysis by utilising the Adomian Decomposition and Taylors series method to obtain the approximate analytical solutions for both substrate and product concentrations, fluxes of the enzymes in the biosensor and provided analytical expressions for the sensitivity and resistance of amperometric biosensor. In [18], authors have considered and analysed a mathematical model of a steady-state amperometric biosensor incorporating the mixed enzyme kinetics with external and internal diffusion limitations under the substrate and product inhibition kinetics. Approximate analytical expressions for the substrate and product concentrations have been provided using the Adomian Decomposition and Taylors series method and the analytical expressions for current, sensitivity and resistance are provided, parameter analysis is also done.

However, this approach is limited to the steady-state conditions of the amperometric biosensor with the substrate inhibition and product inhibition kinetics. To the author's best knowledge, no approximate analytical formulation exists for substrate and product concentrations, current, and biosensor sensitivity in the context of non-steady-state amperometric biosensors operating with mixed enzyme kinetics and subject to internal and mass transfer limitations under substrate and product inhibition kinetics.

This paper aims to present the results of a non-steady-state amperometric biosensor model incorporating mixed enzyme kinetics with substrate and product inhibitions. It was observed that a broad spectrum of concentrations of substrate and product lead to significant variations in both physical and kinetic parameters within the system. Analytical expressions for the mathematical model is particularly preferred over numerical simulations due to their simplicity in manipulation of data and optimizing the critical parameters across a wide range of applications. In this paper, we have provided approximate analytical expressions for non-steady-state substrate and product concentrations as well as current density for all the parameter values of the amperometric biosensor with the mixed enzyme kinetics with the inhibition in substrate and product. The numerical solution is obtained using MATLAB software and subsequently compared with the derived approximate analytical results. Analytical expression for the sensitivity of biosensor is provided. The

limiting cases in the enzymatic kinetics affecting the biosensor working is presented. Also, the analytical expression for effective thickness of the membrane layer for obtaining the maximum current potential is presented.

2 Mathematical Model

Biosnenors generally operate by the Michaelis-Menten reaction, which is given as

$$E + S \underset{k_{-1}}{\overset{k_1}{\rightleftharpoons}} ES \xrightarrow{k_2} E + P \tag{1}$$

where enzyme and substrate are represented as E and S, which react with k_1 kinetics and k_{-1} kinetics for reverse reaction to produce the unstable enzyme substrate complex ES, which then with k_2 kinetics produces enzyme and product P, where the k_i $i = -1, 1, 2$ is the rate constants of reaction. The Michaelis-Menten reaction demonstrates irreversibility in second step due to its unidirectional enzymatic conversion, with electrons flowing from the enzymatic reaction to the electrode as substrate is transformed into product. This irreversibility is a fundamental aspect in biosensor applications, as it ensures the biosensor specificity and sensitivity. The rate at which the product is generated is contingent upon the substrate concentration.

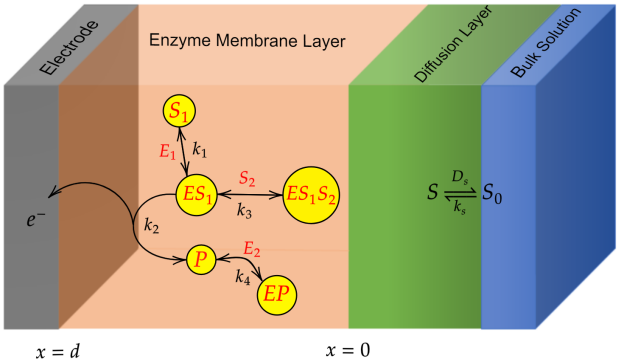

Fig. 1: Illustration of the working of Amperometric biosensor

we consider the non-Michaelis-Menten reaction where the enzyme-substrate complex ES is inhibited and reacts with additional substrate molecule and forms a non-active ESS complex with k_3 kinetics (k_{-3} for backward kinetics), here k_3 and k_{-3} are the rate constant of substrate inhibition

$$ES + S \underset{k_{-3}}{\overset{k_3}{\rightleftharpoons}} ESS \tag{2}$$

Also, this paper examines the inhibition of the product molecule interacting with a molecule of enzyme producing the non-active EP complex with k_4

kinetics (k_{-4} for backward kinetics), here k_4 and k_{-4} are the rate constant of product inhibition

$$E + P \underset{k_{-4}}{\overset{k_4}{\rightleftharpoons}} EP \tag{3}$$

Comprehending the distinct attributes of biosensors is a vital aspect of their design, as depicted in Figure 1. In the bulk solution, the analyte exists and flows to the diffusion layer, where mass transport by diffusion occurs. In the enzyme membrane layer, enzymatic reactions and additional mass transport through diffusion take place. Finally, the analyte reaches the electrode, where electron transfer occurs, leading to the generation of a measurable electrical signal.

The significance of the reversible interactions involving both the substrate and the product often goes unnoticed, even though they constitute a crucial component of the entire process. The following are non-steady non-linear differential kinetics equations of substrate and product inhibition [11]:

$$\frac{\partial s(x,t)}{\partial t} = D_s \frac{\partial^2 s(x,t)}{\partial x^2} - v(s,p), \tag{4}$$

$$\frac{\partial p(x,t)}{\partial t} = D_p \frac{\partial^2 p(x,t)}{\partial x^2} + v(s,p), \quad 0 < x < d \tag{5}$$

where

$$v(s,p) = \frac{V_{max} s(x,t)}{k_m \left(1 + \frac{p(x,t)}{k_p}\right) + s(x,t) \left(1 + \frac{s(x,t)}{k_s}\right)} \tag{6}$$

D_s and D_p represent the diffusion coefficients of the substrate and product concentration, respectively, at the enzyme layer.The concentrations of the substrate and product are represented by the variables $s(x,t)$ and $p(x,t)$, respectively. The parameter V_{max} corresponds to the maximum enzymatic rate, while k_s and k_p are the inhibition constants which is same as k_3 and k_4 in Eqs. (2) and (3). Furthermore, k_m denotes the Michaelis-Menten constant.

$$s(x,0) = 0, \quad p(x,0) = 0 \quad when \quad t = 0, \tag{7}$$

$$\frac{\partial s(0,t)}{\partial x} = 0, \quad p(0,t) = 0 \quad when \quad x = 0, \tag{8}$$

$$s(d,t) = s_0, \quad p(d,t) = 0 \quad when \quad x = d. \tag{9}$$

where s_0 is the concentration of substrate at $x = d$.

The biosensor current density I is expressed as

$$I = n_e F D_p \left.\frac{\partial p}{\partial x}\right|_{x=0} \tag{10}$$

n_e is the amount of electron taking part in the electrochemical reaction. By using the following dimensionless parameters Eqs. (4) and (5) are made

dimensionless.

$$\chi = \frac{x}{d},\ \tau = \frac{D_S t}{d^2},\ S(\chi,\tau) = \frac{s(x,t)}{s_0},\ P(\chi,\tau) = \frac{p(x,t)}{s_0},$$
$$\phi^2 = \frac{V_{max} d^2}{D_s s_0},\ \varphi = \frac{D_p}{D_s},\ \alpha = \frac{s_0}{k_p},\ \gamma = \frac{k_m}{s_0},\ \beta = \frac{s_0^2}{k_s} \tag{11}$$

where $S(\chi,\tau)$ and $P(\chi,\tau)$ depict the dimensionless concentration of the substrate and product. ϕ^2, φ are reaction diffusion parameters, α, β, γ illustrate saturation parameters. τ and χ are dimensionless time and distance.

$$\frac{\partial S(\chi,\tau)}{\partial \tau} = \frac{\partial^2 S(\chi,\tau)}{\partial \chi^2} - \frac{\phi^2 S(\chi,\tau)}{\gamma + \alpha P(\chi,\tau) + S(\chi,\tau) + \beta S^2(\chi,\tau)}, \tag{12}$$

$$\frac{\partial P(\chi,\tau)}{\partial \tau} = \varphi \frac{\partial^2 P(\chi,\tau)}{\partial \chi^2} + \frac{\phi^2 S(\chi,\tau)}{\gamma + \alpha P(\chi,\tau) + S(\chi,\tau) + \beta S^2(\chi,\tau)}. \tag{13}$$

with the following boundary conditions:

$$S(\chi,0) = 0,\ P(\chi,0) = 0 \quad when \quad \tau = 0, \tag{14}$$
$$\frac{\partial S(0,\tau)}{\partial \chi} = 0,\ P(0,\tau) = 0 \quad when \quad \chi = 0, \tag{15}$$
$$S(1,\tau) = 1,\ P(1,\tau) = 0 \quad when \quad \chi = 1. \tag{16}$$

the dimensionless current is as follows:

$$\Psi = \frac{I}{n_e F D_p}\left[\frac{d}{s_0}\right] = \left.\frac{\partial P(\chi,\tau)}{\partial \chi}\right|_{\chi=0} \tag{17}$$

3 Approximate analytical expressions of non - steady - state substrate and product concentrations and current using HPM

In fields like applied mathematics, physics and chemical engineering, problems are depicted using non-linear equations. Finding solutions for these non-linear differential equations is the constant problem faced by scientists in those fields. In recent years, various analytical and semi-analytical techniques have gained considerable attention for solving strongly nonlinear differential equations in physical, biological, and chemical sciences. These methods include the Homotopy analysis method (HAM) [19], Taylor's series method (TSM) [20]-[23], Homotopy perturbation method (HPM) [13], [24]-[28], Variational iteration method (VIM) [29]-[32], and Adomian decomposition method (ADM) [33]-[35].

Ji-Huan He introduced the Homotopy perturbation method (HPM) [13] as a technique for obtaining approximate analytical solutions for various strongly

non-linear differential equations. Recently, J.H. He and his colleagues [24] have applied the HPM to solve problems arising in oscillators, while Vijayalakshmi and Senthamarai [25] have utilized the method to solve a non-linear prey-predator model and Rajendran et al made use of the HPM to obtain approximate analytical expressions for non-linear steady [26] and non-steady state [27] amperometric biosensor models and packed bed reactors model [28]. The HPM offers an advantage over other approximate analytical methods by reducing the inherent complexity of solving non-linear differential equations. Approximate analytical solution of substrate concentration Eq. (12) derived using HPM (see Appendix - A) is obtained as follows:

$$S(\chi,\tau) = \frac{\cosh\left(\sqrt{\delta}\chi\right)}{\cosh(\sqrt{\delta})} - \sum_{n=0}^{\infty} \frac{(2n+1)\, e^{-\eta\tau} \cos\left(\frac{(2n+1)\pi}{2}\chi\right)}{\eta \sin\left(\frac{(2n+1)\pi}{2}\right)} \tag{18}$$

approximate analytical solution of product concentration Eq. (13) derived using the HPM is obtained as:

$$\begin{aligned} P(\chi,\tau) = {} & \frac{\chi}{\varphi} + \frac{1-\chi-\cosh(\sqrt{\delta}\chi)}{\varphi\cosh(\sqrt{\delta})} \\ & + \delta\pi \sum_{n=0}^{\infty} \frac{(-1)^n(2n+1)}{\eta[\delta\varphi-\eta(\varphi-1)]} \times \left[\frac{\sin(\sqrt{\eta/\varphi}(\chi-1))}{\sin(\sqrt{\eta/\varphi})} + \cos\left((2n+1)\frac{\pi}{2}\chi\right)\right] e^{-\eta\tau} \\ & - \frac{2\delta}{\pi} \sum_{n=1}^{\infty} \frac{(-1)^n}{n[\delta\varphi - n^2\pi^2\varphi(\varphi-1)]} \times \left[\frac{\sin[n\pi(\chi-1)]}{\cosh(\sqrt{\delta - n^2\pi^2\varphi})} - \sin(n\pi\chi)\right] e^{-n^2\pi^2\varphi\tau} \\ & + \frac{(\varphi-1)}{\varphi}\left[\frac{2\sin(\sqrt{[\delta/(\varphi-1)]}(\chi-1))}{\sin(2\sqrt{[\delta/(\varphi-1)]})} - \frac{\sin(\sqrt{[\delta/(\varphi-1)]}\chi)}{\sin(\sqrt{[\delta/(\varphi-1)]})}\right. \\ & \left. + \frac{\cos(\sqrt{[\delta/(\varphi-1)]}\chi)}{\cos(\sqrt{[\delta/(\varphi-1)]})}\right] e^{-\frac{\delta\varphi}{1-\varphi}\tau} \end{aligned} \tag{19}$$

where

$$\eta = \frac{\pi^2(2n+1)^2}{4} + \delta, \quad \delta = \frac{\phi^2}{\alpha\,(\gamma/\alpha + 1/\alpha\ + \beta/\alpha)} \tag{20}$$

Eqs. (18) and (19) satisfies the given boundary conditions (14) - (16) and we obtain dimensionless current given by Eq. (17) as

$$\begin{aligned} \Psi = \frac{I(\tau)}{n_e F D_p}\left[\frac{d}{s_0}\right] = {} & \left[\frac{1}{\varphi} - \frac{1}{\varphi\cosh(\sqrt{\delta})}\right] \\ & + \delta\pi \sum_{n=0}^{\infty} \left[\frac{(-1)^n(1+2n)\cot(\sqrt{\eta/\varphi})}{\sqrt{\eta\varphi}[\delta\varphi-\eta(\varphi-1)]}\right] e^{-\eta\tau} \end{aligned}$$

$$+ 2\delta \sum_{n=1}^{\infty} \left[\frac{(-1)^n - \sec(\sqrt{\delta - n^2\pi^2})}{\delta\varphi - n^2\pi^2\varphi(\varphi - 1)} \right] e^{-n^2\pi^2\varphi\tau} \tag{21}$$

3.1 Limiting cases

3.1.1 First-Order (unsaturated) kinetics

We first discuss a limitation that arises when the Michaelis-Menten constant k_i exceeds the amount of substrate available in the enzyme layer $S(\chi, \tau)$ i.e $S \ll k_i$ where $i = s, p, m$. Hence the Eqs. (12) and (13) is reduced as

$$\frac{\partial S(\chi,\tau)}{\partial \tau} = \frac{\partial^2 S(\chi,\tau)}{\partial \chi^2} - \frac{\phi^2}{\gamma} S(\chi,\tau) \tag{22}$$

$$\frac{\partial P(\chi,\tau)}{\partial \tau} = \varphi \frac{\partial^2 P(\chi,\tau)}{\partial \chi^2} + \frac{\phi^2}{\gamma} S(\chi,\tau) \tag{23}$$

The above represented Eqs. (22) and (23) are linear partial differential equation for which we can obtain the exact solutions. By solving the above equations the substrate and product concentrations and the biosensor current are obtained identical to the Eqs. (18), (19) and (21) but $\delta = \phi^2/\gamma$

3.1.2 Zero-Order (saturated) kinetics

We examine another significant constraint involving substrate concentration $S(\chi, \tau)$ exceeding the Michaelis-Menten kinetics k_i in the enzymatic layer i.e. $S \gg k_i$ where $i = s, p, m$. Hence the Eqs. (12) and (13) is reduced as

$$\frac{\partial S(\chi,\tau)}{\partial \tau} = \frac{\partial^2 S(\chi,\tau)}{\partial \chi^2} - \phi^2 \tag{24}$$

$$\frac{\partial P(\chi,\tau)}{\partial \tau} = \varphi \frac{\partial^2 P(\chi,\tau)}{\partial \chi^2} - \phi^2 \tag{25}$$

The solution of the substrate and product concentration of zero order kinetics by solving the above equations is obtained as

$$S(\chi,\tau) = 1 + \frac{\phi^2}{2}(\chi^2 - 1) - \frac{4}{\pi} \sum_{n=0}^{\infty} \left(\frac{4\phi^2}{\pi^2(2n+1)^2} - 1 \right) \times \frac{\cos\left(\frac{(2n+1)\pi}{2}\chi\right) e^{-\eta\tau}}{(2n+1)\,\sin\left(\frac{(2n+1)\pi}{2}\right)} \tag{26}$$

$$P(\chi,\tau) = \frac{\phi^2}{2\varphi}(\chi - \chi^2) + \frac{2\phi^2}{\varphi\pi^3} \sum_{n=1}^{\infty} \frac{\sin(n\pi x)}{n^3} \left[(-1)^n - 1\right] e^{-n^2\pi^2\varphi\tau} \tag{27}$$

and the current expression is obtained as

$$\Psi = \frac{\phi^2}{2\varphi} + \frac{2\phi^2}{\varphi} \sum_{n=1}^{\infty} \frac{\left((-1)^n - 1e^{-n^2\pi^2\varphi\tau}\right)}{n^2\pi^2} \tag{28}$$

the above Eqs. (26), (27) and (28) are the analytical expressions of the substrate Eq. (24) and product Eq. (25) concentrations and current.

4 Approximate analytical expressions of steady - state substrate and product concentrations and current using HPM

Biosensor reaches its equilibrium and attains a steady-state over an extended period of time as τ approaches infinity. In this state, the system's dynamics become independent of time, and the system has achieved a stable, unchanging configuration.
The steady-state analytical expressions of dimensionless concentrations of the substrate and product can be obtained by evaluating Eqs. (18) - (19) as $\tau \to \infty$, given as follows:

$$S(\chi) = \frac{\cosh\left(\sqrt{\delta}\chi\right)}{\cosh(\sqrt{\delta})} \tag{29}$$

$$P(\chi) = \frac{\chi}{\varphi} + \frac{1 - \chi - \cosh(\sqrt{\delta}\chi)}{\varphi\cosh(\sqrt{\delta})} \tag{30}$$

the steady-state dimensionless current is obtained by evaluating Eq. (21) as

$$\Psi = \frac{I}{n_e F D_p}\left[\frac{d}{s_0}\right] = \left[\frac{1}{\varphi} - \frac{1}{\varphi\cosh(\sqrt{\delta})}\right] \tag{31}$$

Previously [18] we have derived approximate analytical solution for the steady-state condition of amperometric biosensor with substrate inhibition and product inhibition kinetics using TSM and ADM. Eqs. (29) and (30) provide new approximate analytical solution for the concentrations of substrate and product of amperometric biosensor with substrate inhibition and product inhibition kinetics.

5 Validation of analytical results

In order to validate the accuracy of the approximate analytical solution obtained using HPM for non-steady-state conditions, we employed the pdepe tool in Matlab software to obtain the numerical solution. The pdepe utilizes the method of lines (MOL) to solve time-dependent partial differential equations (PDEs). MOL discretizes the spatial variables while treating the time variable

analytically, effectively converting the PDE into a system of ordinary differential equations (ODEs). It automatically manages the spatial discretization and selects the suitable ODE solver for the given problem.

The results were then compares and presented in Figs. 2 and 5 and Table 1 - 3. The comparison revealed that the analytical solution obtained using HPM was satisfactory the maximum error percentage noted between the numerical and non-steady-state approximate analytical solution is 0.078%. In addition, we have compared the novel steady-state approximate analytical solution Eqs. (29) and (30) using HPM with the previous results obtained in [18]. From the Table 2 it is scene that the approximate analytical result obtained using the HPM gives better result for our system compared to the previous result. The maximum error obtained between the analytical and numerical solution for steady-state condition is found to be 0.024% which is lesser than the previous result.

The comparison of the dimensionless current response is also presented in Table 3. The comparison revealed that the analytical solution obtained using HPM was satisfactory for the dimensionless current of the amperometric biosensor with substrate and product inhibition kinetics. The maximum error percentage obtained between the numerical solution and current response obtained analytically using HPM is 0.32%.

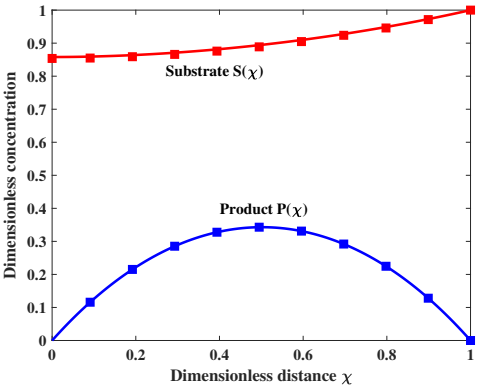

Fig. 2: Concentration profiles of substrate Eq. (18) and product Eq. (19) in dimensionless form are depicted as a function of distance from the electrode (χ) for the parameter values $\tau = 10$, $\phi^2 = 1$, $\alpha = 2$, $\beta = 3$, $\gamma = 1$ and $\varphi = 0.1$ where '—' represents the numerical solution and ■ represents the HPM solution.

6 Result and discussion

Eqs. (18) and (19) present new closed-form approximate analytical expressions for the non-steady-state substrate and product concentrations, Eqs.

(12) and (13), respectively, of the amperometric biosensor model with substrate inhibition and product inhibition. Similarly, Eqs. (29) and (30) provide approximate analytical expressions for the steady-state concentrations of the substrate and product. Finally, Eq. (21) and Eq. (31) describe the analytical expressions for the non-steady-state and steady-state current, respectively.

Fig. 2 represents the dimensionless concentration of substrate S and product P of the non-Michaelis-Menten reaction kinetics model of the amperometric biosensor with substrate and product inhibition. From the figure, it is observed that the substrate concentration is a increasing function. By the boundary condition Eq. (16) the substrate reaches its maximum concentration at $\chi = 1$ it can be observed that the from the initial point $\chi = 0$ substrate concentration increases gradually and reaches its maximum concentration when $\chi = 1$. Whereas, the product concentration initially increases from 0 and reaches its peak concentration as the χ approaches the 0.5 away from the surface of the electrode and it gradually decreases to 0 concentration when $\chi = 1$ equivalent to the boundary condition Eq. (16) for all values of other parameters.

Figs. 3 and 4 represents the effect of dimensionless time τ and dimensionless distance χ on the concentrations of substrate and product. From the figures it is observed that both the concentrations are decreasing functions with respect to time this phenomenon can be clearly seen in Figs. 3b and 4b. The concentration attains is at its maximum at the initial stage of the dimensionless time and then gradually decreases as the time increases. This can be clearly seen in Fig. 5, it is seen that time is inversely proportional to the concentrations. From Figs. 5a and 5b it is seen that the concentration decreases as time increases and attains its equilibrium when the time $\tau \geq 2$ and there is no change in the concentrations of substrate and product.

From the graphs of the dimensionless current presented in Fig. 6 - 9, it can be observed that the current stabilizes instantly when $\tau > 1$ for all parameter values. When the saturation parameters β and γ are increased, the current decreases, as shown in Figs. 6 and 7. Where as in the case of ratio of diffusion coefficient φ the current decreases with the increase of the parameter this can be seen in Fig. 8. When $\tau = 1$ the current reaches its maximum and then when dimensionless time $\tau = 2$ the current gradually decreases and stabilizes when $\tau = 3$. However, Figs. 9 indicates that the current increases with an increase in the diffusion parameter ϕ^2. The saturation parameter α does not have any significant effect on the current response of amperometric biosensor.

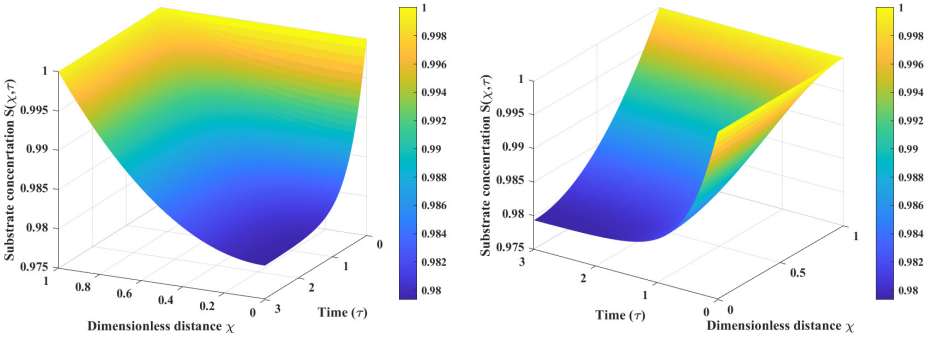

(a) (b)

Fig. 3: Simulation of substrate concentration versus dimensionless time τ and dimensionless distance χ for the parametric values $\phi^2 = 0.5,\ \alpha = 2,\ \beta = 5,\ \gamma = 0.1,\ \varphi = 0.6$.

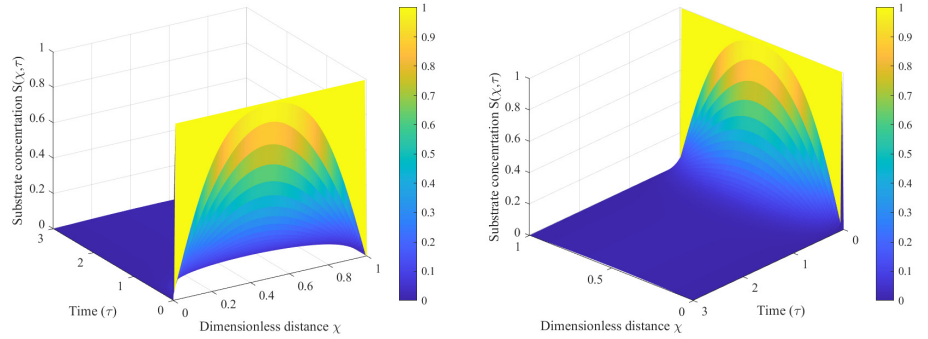

(a) (b)

Fig. 4: Simulation of product concentration versus dimensionless time τ and dimensionless distance χ for the parametric values $\phi^2 = 0.5,\ \alpha = 2,\ \beta = 5,\ \gamma = 0.1,\ \varphi = 0.6$.

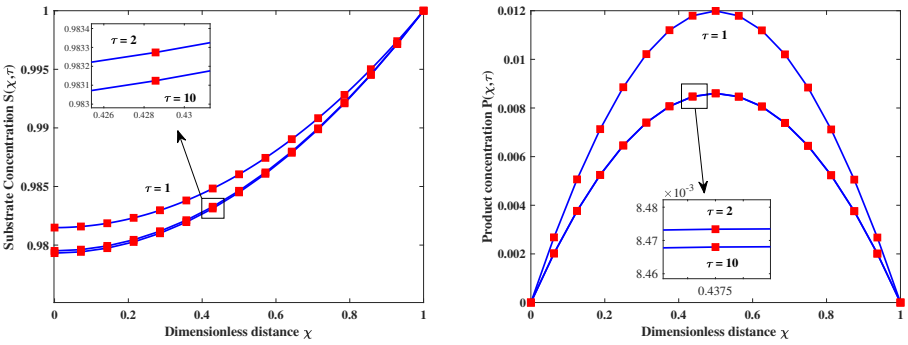

(a) (b)

Fig. 5: Non-steady-state concentrations of (5a) substrate and (5b) product versus dimensionless distance χ with variation in dimensionless time τ for the fixed parametric values $\phi^2 = 0.5,\ \alpha = 2, \beta = 5,\ \gamma = 0.1,\ \varphi = 0.6$, where '$-$' represents numerical and '■' represents the HPM solution.

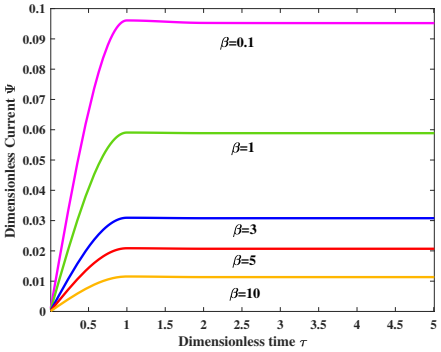

Fig. 6: Dimensionless current Ψ as a function of dimensionless time (τ) for fixed $\phi^2 = 0.5,\ \alpha = 2,\ \gamma = 0.1,\ \varphi = 1$ and for different values of β

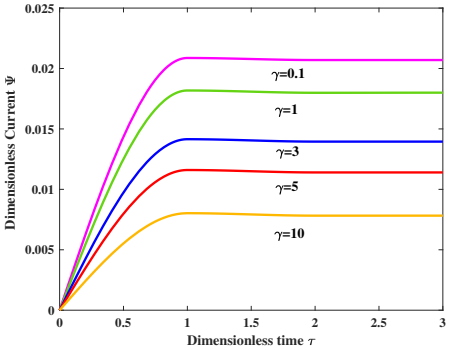

Fig. 7: Dimensionless current Ψ as a function of dimensionless time (τ) for fixed $\phi^2 = 0.5,\ \alpha = 2,\ \beta = 5,\ \varphi = 1$ and for different values of γ

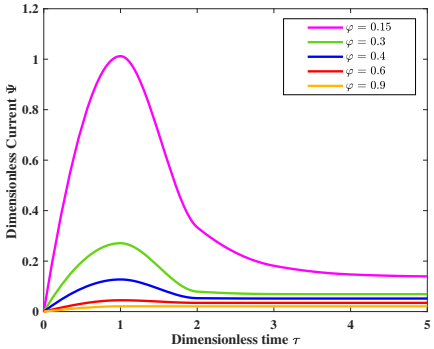

Fig. 8: Dimensionless current Ψ as a function of dimensionless time (τ) for fixed $\phi^2 = 0.5,\ \alpha = 2,\ \beta = 5,\ \gamma = 0.1$ and for different values of φ

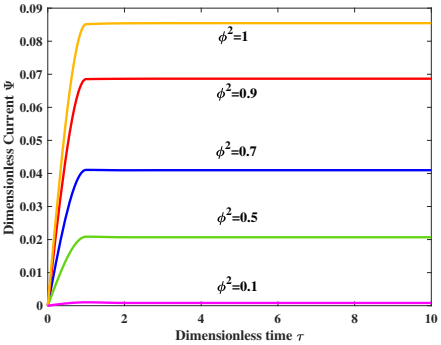

Fig. 9: Dimensionless current Ψ as a function of dimensionless time (τ) for fixed $\alpha = 2,\ \beta = 5,\ \gamma = 0.1,\ \varphi = 1$ and for different values of ϕ^2

Table 1: Table presenting a comparison between the numerical solution for the non-steady-state substrate $S(\chi)$ and product $P(\chi)$ concentration and the analytical solution obtained through the HPM for the fixed parameters $\tau = 10, \phi^2 = 0.74$, $\alpha = 2$, $\beta = 5$, $\gamma = 0.1$, and $\varphi = 1$

	$S(\chi)$			$P(\chi)$		
χ	Numerical	HPM	Error%	Numerical	HPM	Error
0.0	0.96960	0.97030	0.07219	0.00000	0.00000	0.00000
0.2	0.97083	0.97081	0.00185	0.04858	0.04852	0.12351
0.4	0.97449	0.97609	0.16371	0.07276	0.07266	0.13156
0.6	0.98058	0.98165	0.10883	0.07269	0.07260	0.12022
0.8	0.98909	0.99026	0.11868	0.04844	0.04842	0.04129
1.0	1.00001	1.00000	0.00093	0.00000	0.00000	0.00000
Average Error%			0.07677			0.06943

6.1 Sensitivity

Sensitivity is a pivotal attribute of amperometric biosensor. The sensitivity of the biosensor can be defined as the rate of change of the steady-state current concerning the variations of substrate concentration. Because of the significant variations in both biosensor current and substrate concentration, particularly when making comparisons between different sensors, another valuable parameter to consider is the dimensionless sensitivity. The sensitivity of the amperometric biosensor with the substrate inhibition and product inhibition kinetics to changes in substrate concentration is calculated using Eq.

Table 2: Table presenting a comparison between the numerical solution for the steady-state substrate $S(\chi)$ and product $P(\chi)$ concentrations, and our prior findings as reported in reference [18], alongside the current result Eq. (29). This analysis is conducted under constant experimental parameters: $\phi_1^2 = 1$, $\phi_2^2 = 0.3$, $\gamma = 0.5$, $\alpha = 10$, $\beta = 1$ for $S(\chi)$ and $\phi_1^2 = 1$, $\phi_2^2 = 1$ $\alpha = 3$, $\beta = 5$, $\gamma = 2$ for $P(\chi)$

	$S(\chi)$							$P(\chi)$						
χ	Numerical	TSM[18]	error%[18]	ADM[18]	error%[18]	HPM	error %	Numerical	TSM[18]	error%[18]	ADM[18]	error%[18]	HPM	error%
0.0	0.80540	0.80500	0.04966	0.81220	0.84430	0.80530	0.01242	0.00000	0.00000	0.00000	0.00000	0.00000	0.00000	0.00000
0.2	0.81315	0.81269	0.05707	0.81935	0.76222	0.81280	0.04317	0.00256	0.00256	0.13580	0.00255	0.38356	0.00256	0.03908
0.4	0.83648	0.83602	0.05548	0.84168	0.62118	0.83635	0.01572	0.00383	0.00383	0.09064	0.00382	0.36035	0.00384	0.05217
0.6	0.87538	0.87498	0.04571	0.87918	0.43342	0.87516	0.02549	0.00383	0.00383	0.09069	0.00382	0.36054	0.00383	0.05220
0.8	0.92986	0.92959	0.02927	0.93186	0.21424	0.92965	0.02265	0.00255	0.00255	0.13612	0.00254	0.38446	0.00255	0.07834
1.0	0.99992	0.99984	0.00802	0.99971	0.02098	0.99994	0.00179	0.00000	0.00000	0.00000	0.00000	0.00000	0.00000	0.00000
Average error %			0.04087		0.47573		0.01961			0.07554		0.24815		0.02394

Table 3: Table comparing the numerical solution of the current response with the analytical solution obtained using HPM Eq. (21) with change in time. The fixed values are $\phi^2 = 0.5$, $\alpha = 2$, $\beta = 5$, $\gamma = 0.1$ and for different values of φ

	$\varphi = 0.1$			$\varphi = 0.5$			$\varphi = 1$		
τ	Numerical	HPM	error%	Numerical	HPM	error%	Numerical	HPM	error%
0	0.00000	0.00000	0.00000	0.00000	0.00000	0.00000	0.00000	0.00000	0.00000
1	1.61900	1.61300	0.37060	0.06955	0.06933	0.31632	0.02087	0.02083	0.19166
2	0.72550	0.72380	0.23432	0.04154	0.04132	0.52961	0.02070	0.02067	0.14493
3	0.39680	0.39570	0.27722	0.04135	0.04127	0.19347	0.02070	0.02067	0.14493
4	0.27560	0.27520	0.14514	0.04135	0.04127	0.19347	0.02070	0.02067	0.14493
5	0.23100	0.22900	0.86580	0.04135	0.04127	0.19347	0.02070	0.02067	0.14493
Average error%			0.31551			0.23772			0.12856

(31).

$$B_A = \frac{\partial I(s_0)}{\partial s_0} \times \frac{s_0}{I(s_0)} = \frac{\left(D_s \; s_0 \; \sinh\left(\sqrt{\delta}\right) \times \left(\frac{\delta}{s_0} - \frac{\phi^2 \left(k_p / s_0^2 + k_p / k_s k_m \right)}{\alpha (1/\alpha + \beta/\alpha + \gamma/\alpha)^2} \right) \right)}{2 \; D_p \; \sqrt{\delta} \; \cosh\left(\sqrt{\delta}\right)^2 \left(\frac{1}{\varphi} - \frac{1}{\varphi \cosh\left(\sqrt{\delta}\right)} \right)} \tag{32}$$

where B_A is the sensitivity of the biosensor.

Fig. 10 - 13 represents the non-monotonic sensitivity of biosensor B_A for increasing substrate concentration s_0. It is noted that the increase in the concentration decreases the sensitivity of the amperometric biosensor. When $s_0 \approx 10^3 \mu M$, the biosensor sensitivity reduces to its minimum value 0. An increase in the enzyme layer distance d and the maximum enzymatic rate V_{max} results increase of the sensitivity B_A which can be seen in Figs. 10 and 13. Whereas in the case of the diffusion constants D_s, D_p and rate constant k_m, the biosensor sensitivity of the maximum enzymatic rate results in a decrease of the sensitivity B_A as represented in Figs. 11 and 12.

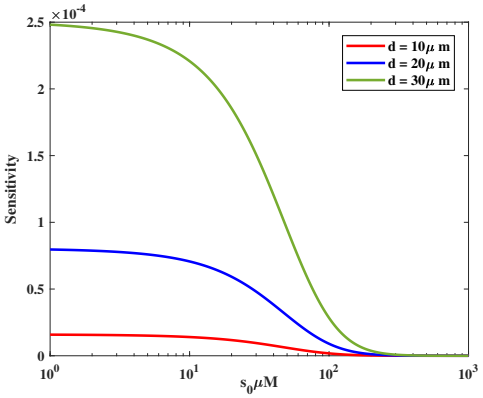

Fig. 10: Sensitivity of biosensor B_A Eq. (32) versus $s_0 \mu M$ for fixed values of $V_{max} = 1 \mu M/s$, $k_s = 100M$, $k_m = 100M$, $k_p = 100M$, $D_s = D_p = 100 \mu m^2/s$ and for various valued of distance d

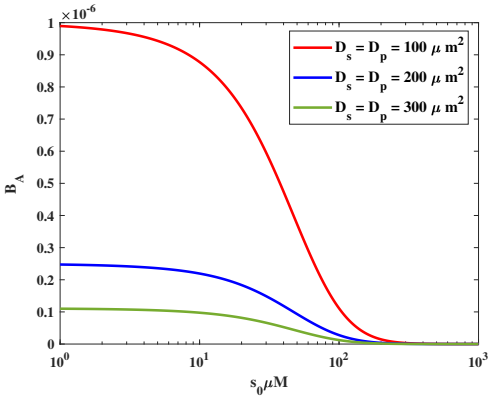

Fig. 11: Sensitivity of biosensor B_A Eq. (32) versus $s_0\mu M$ for fixed values of $V_{max} = 1\mu M/s,\ k_s = 100M,\ k_m = 100M,\ k_p = 100M,\ d = 10\mu m$ and for various valued of distance D_s and D_p

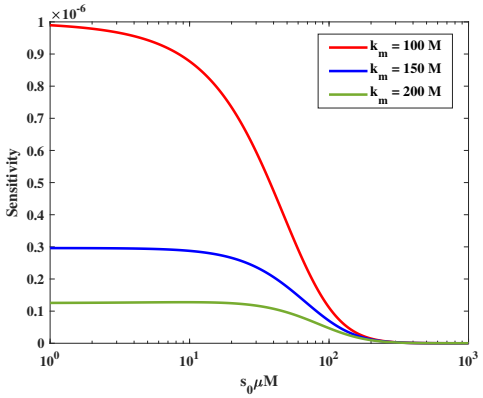

Fig. 12: Sensitivity of biosensor B_A Eq. (32) versus $s_0\mu M$ for fixed values of $V_{max} = 1\mu M/s,\ k_s = 100M,\ d = 10\mu m,\ k_p = 100M,\ D_s = D_p = 100\mu m^2/s$ and for various valued of distance k_m

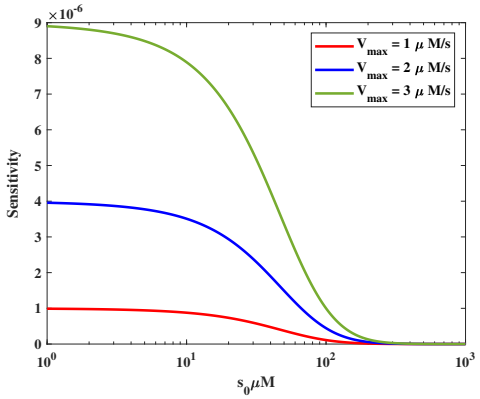

Fig. 13: Sensitivity of biosensor B_A Eq. (32) versus $s_0\mu M$ for fixed values of $k_s = 100M,\ k_m = 100M,\ d = 10\mu m,\ k_p = 100M,\ D_s = D_p = 100\mu m^2/s$ and for various valued of distance V_{max}

6.2 Effective membrane thickness

By making use of the dimensionless current Eq. (31), the approximate value of the effective membrane thickness d can be determined analytically. This value corresponds to the point at which the steady-state current reaches its maximum, given specific parameter values of $V_{max},\ D_s,\ K_m,\ K_p,\ K_s,\ s_0$. Current equation Eq. (31) can be written as follows:

$$\frac{I(d)}{n_e F} = \frac{D_s s_0}{d}\left[1 - \operatorname{sech}(\sqrt{\delta})\right] \tag{33}$$

by differentiating the above equation with respect to d we obtain the expression as follows

$$\frac{\partial I(d)}{\partial d} = \frac{n_e F D_s s_0}{d^2}\left[\frac{\sqrt{\delta}\tanh(\sqrt{\delta}) - \cosh(\sqrt{\delta}) + \cosh(\sqrt{\delta})\operatorname{sech}(\sqrt{\delta})}{\cosh^2(\sqrt{\delta})}\right] \tag{34}$$

and we aim to find the value of d when the derivative reaches zero

$$\sqrt{\delta}\tanh(\sqrt{\delta}) - 2\sinh^2(\sqrt{\delta}/2) = 0 \tag{35}$$

The numerical solution of Eq. (35) results in a singular value of $\delta_{max} \approx 1.5055$. As a result, we can determine the membrane thickness d at which the maximum current I is achieved, where

$$d_{max} = \delta_{max}\sqrt{\frac{D_s k_m s_0\left(\frac{k_p}{s_0} + \frac{k_p}{k_m} + \frac{s_0 k_p}{k_s k_m}\right)}{V_{max} k_p}} = 86.87\mu m \tag{36}$$

at the parametric values $D_s = 300\mu m^2/s, k_m = 100M, k_p = 100M, k_s = 100M, V_{max} = 10\mu M/s, s_0 = 10\mu M$.

7 Conclusion

The mathematical model of amperometric biosensor with the inhibitions of substrate and product is discussed in this paper. The model is a non-linear non-steady-state reaction-diffusion equation of second order. The closed-form approximate analytical expressions for substrate and product concentrations obtained using the Laplace transform and HPM method for non-steady and steady-state system. The obtained approximate analytical solutions are compared with the numerical solution obtained by using MATLAB software. The limiting cases of the enzyme kinetics on the amperometric biosensor is also analysed and the analytical expressions for the both cases are derived and presented.

In addition, the analytical expressions of Biosensor current and sensitivity are also presented. It is noted that the diffusion coefficient ratio φ has a significant impact on the biosensor current as it peaks when dimensionless time $\tau = 1$ then starts decreasing gradually and stabilizes only when $\tau = 3$ where as the other parameters stabilizes instantly after $\tau = 1$. The bulk substrate concentration s_0 has a significant impact on the sensitivity of amperometric biosensor. The expression for calculating effective membrane thickness for which the maximum current can be obtained for the given specific parameter values is represented as $d_{max} = 1.5055\sqrt{D_s k_m s_0 \left(\frac{k_p}{s_0} + \frac{k_p}{k_m} + \frac{s_0 k_p}{k_s k_m}\right)/V_{max} k_p}$. The theoretical model represented in this paper will be helpful for the experimental scientists to improve the sensitivity of amperometric biosensor and a better understanding of the characteristics of substrate and product inhibitions in amperometric biosensor.

Appendix A Obtaining an Approximate Analytical Solution of the Equation through HPM.

The homotopy for Eq. (12) is constructed as follows:

$$(1-p)\left[\frac{\partial S(\chi,\tau)}{\partial \tau} - \frac{\partial^2 S(\chi,\tau)}{\partial \chi^2} + \frac{\phi^2 S(\chi,\tau)}{\alpha(\gamma/\alpha + 1/\alpha + \beta/\alpha)}\right] + p\left[\frac{\partial S(\chi,\tau)}{\partial \tau} - \frac{\partial^2 S(\chi,\tau)}{\partial \chi^2} + \frac{\phi^2 S(\chi,\tau)}{\gamma + \alpha P(\chi,\tau) + S(\chi,\tau) + \beta S^2(\chi,\tau)}\right] = 0 \quad \text{(A1)}$$

The given conditions at the initial and boundaries of Eq. (A1) are

$$\begin{aligned} &At\ \tau = 0,\ S(\tau,0) = 0, \\ &At\ \chi = 0,\ \tfrac{\partial S(0,\tau)}{\partial \chi} = 0, \end{aligned} \quad \text{(A2)}$$

$$At \;\; \chi = 1, \;\; S(1,\tau) = 1$$

Approximate solution of the above Eq. (A1) is [13]

$$S(\chi,\tau) = S_0(\chi,\tau) + pS_1(\chi,\tau) + p^2 S_2(\chi,\tau) + p^3 S_3(\chi,\tau) + \cdots \tag{A3}$$

By substituting Eq. (A3) into Eq. (A1) and equating the coefficients of the zeroth power of p, we obtain

$$\frac{\partial S_0(\chi,\tau)}{\partial \tau} - \frac{\partial^2 S_0(\chi,\tau)}{\partial \chi^2} + \delta S_0(\chi,\tau) = 0 \tag{A4}$$

where

$$\delta = \frac{\phi^2}{\alpha(1/\alpha \; + \gamma/\alpha + \beta/\alpha)}$$

The given conditions at the initial and boundaries are defined by.

$$\begin{aligned} &At \;\; \tau = 0, \;\; S_0(\chi,0) = 0, \\ &At \;\; \chi = 0, \;\; \tfrac{\partial S_0(0,\tau)}{\partial \tau} = 0, \\ &At \;\; \chi = 1, \;\; S_0(1,\tau) = 1 \end{aligned} \tag{A5}$$

We can express the Eqs. (A4) and (A5) in the Laplace domain as follows [36]:

$$\frac{d^2 \widetilde{S}_0(\chi,s)}{d\chi^2} - (s+A)\,\widetilde{S}_0(\chi,s) = 0, \tag{A6}$$

the boundary conditions are specified as

$$\begin{aligned} &when \;\; \chi = 0, \;\; \tfrac{d\widetilde{S}_0(\chi,s)}{d\chi} = 0, \\ &when \;\; \chi = 1, \;\; \widetilde{S}_0(\chi,s) = \tfrac{1}{s}. \end{aligned} \tag{A7}$$

the Laplace transformation of $S_0(\chi,\tau)$ is denoted as $\widetilde{S}_0(\chi,s)$, where s is the Laplace variable. By using Eq. (A7), the solution of $\widetilde{S}_0$ can be obtained as shown in Eq. (A8).

$$\widetilde{S}_0(\chi,\tau) = \frac{\cosh\left(\sqrt{s+\delta}\chi\right)}{\cosh(\sqrt{s+\delta})} \tag{A8}$$

The concentration of substrate $S(\chi,\tau)$ can be obtained by utilizing the complex inversion formula we get the approximate analytical expression for the concentration of the substrate $S(\chi,\tau)$ which is the result given in Eq. (18). Similarly, we can get the approximate analytical expression of the product concentration Eq. (13).

Appendix B Nomenclature

Symbol	Meaning	Unit
s	Concentration of substrate	μM
p	Concentration of product	μM
s_0	Concentration of substrate at $x = d$	μM
t	Time	s
k_m	Michaelis-menten constant	M
k_s, k_p	Inhibition constants	M
V_{max}	Maximal enzymatic rate	$\mu M/s$
d	Thickness of the enzyme layer	μm
F	Faraday constant	C/mol
D_s	Diffusion coefficient of the substrate	$\mu m^2/s$
D_p	Diffusion coefficient of the product	$\mu m^2/s$
I	Density of the current	$\mu A/cm^2$
x	Distance	cm
n_e	Number of electrons take part in electrochemical reaction	None
S	Dimensionless substrate concentration	None
P	Dimensionless product concentration	None
χ	Dimensionless distance	None
τ	Dimensionless time	None
ϕ^2	Diffusion parameter of substrate	None
φ	Ratio of diffusion coefficient	None
α	Saturation parameter	None
β	Saturation parameter	None
γ	Saturation parameter	None
B_A	Sensitivity of biosensor	None

Acknowledgments. The authors are very much thankful to the management, SRM Institute of Science and Technology for their continuous support and encouragement.

Declarations

Funding This research did not receive any specific grant from funding agencies in the public, commercial, or not-for-profit sectors.

Conflict of interest The authors declare that they have no conflict of interest.

Authors' contributions M. Mallikarjuna wrote the main manuscript text, prepared figures, did the formal analysis, methodology and prepared figures, and R. Senthamarai did conceptualization, methodology, supervision, investigation, provided resources, validation and visualization.

References

[1] K. Habermüller, M. Mosbach, W. Schuhmann, Fresenius' J. Anal. Chem. 366, 560 (2000)

[2] E. Lojou, P. Bianco, J. Electroceramics 16, 79 (2006)

[3] B. D. Malhotra, A. Chaubey, Sensors and Actuators B: Chemical 91(1-3) 117 (2003)

[4] N. P. Revsbech, M. Nielsen, D. Fapyane, Sensors 20 (15) 4326 (2020)

[5] M. I. Prodromidis, M. I. Karayannis, Electroanalysis: An International Journal Devoted to Fundamental and Practical Aspects of Electroanalysis 14.4 241 (2002)

[6] H. Gutfreund, Kinetics for the Life Sciences (Cambridge University Press, Cambridge, 1995)

[7] F.W. Scheller, F. Schubert, Biosensors (Elsevier Science, Amsterdam, 1992)

[8] S. Meric, O. Tunay, S.H. Ali, Environ. Technol. 23(2), 163 (2002)

[9] J. Mirón, M.P. González, J.A. Vázquez, L. Pastrana, M.A. Murado, Enzyme Microb. Technol. 34(5), 513 (2004)

[10] J. Kulys, R. Baronas, Sens. 6(11), 1513 (2006)

[11] D. Šimelevičius, R. Baronas, J. Math Chem. 47(1), 430 (2010)

[12] A. Meena, L. Rajendran., J. Electroanal. Chem. 644(1), 50 (2010)

[13] J. H. He, App. Math. and comp. 135(1), 73-79 (2003)

[14] P. Manimozhi, A. Subbiah, L. Rajendran, Sensors and Actuators B: Chemical. 147(1), 290 (2010)

[15] R. Senthamarai, R. Jana Ranjani, Phy. Conf. Series. 1000 (2018)

[16] R. Swaminathan, M. C. Devi, L. Rajendran, K. Venugopal, J. Electroanal. Chem. 895, 115527 (2021)

[17] R. U. Rani, L. Rajendran, M. E. Lyons, J. Electroanal. Chem. 886, 115103 (2021)

[18] M. Mallikarjuna, R. Senthamarai, Journal of Electroanal. Chem. 946, 117699. (2023)

[19] G. Suganya, R. Senthamarai, CRM. 14, 1093 (2022)

[20] M. Sivakumar, R. Senthamarai, L. Rajendran, M. E. G. Lyons, Int. J. Electrochem. Sci. 17, 221159 (2022)

[21] M. Sivakumar, R. Senthamarai, L. Rajendran, M. E. G. Lyons, Int. J. Electrochem. Sci. 17, 221031 (2022)

[22] C. H. He, Y. Shen, F. Y. Ji, Fractals. 28, 2050011 (2022)

[23] S. Vinolyn Sylvia, R. Joy Salomi, L. Rajendran, M. Abukhaled, J. Math. Chem. 59, 1332 (2021)

[24] J. H. He, M. L. Jiao, K. A. Gepreel, Y. Khan, Math. and Computers in Simul. 204, 243 (2023)

[25] T. Vijayalakshmi, R. Senthamarai, Eng. Lett. 30(4), 1684 (2022)

[26] R. J. Salomi, S. V. Sylvia, L. Rajendran, M. E. G. Lyons, J. Electroanal. Chem, 895, 115421 (2021)

[27] R. J. Salomi, S. V. Sylvia, L. Rajendran, J. Electroanal. Chem. 928, 117067 (2023)

[28] V. M. PonRani, L. Rajendran, J. Math Chem. 50(5), 1333 (2012)

[29] Suganya G, Senthamarai R, J. Appl. Nonlinear Dyn, 11, 741 (2022)

[30] P. Manimozhi, A. Subbiah, L. Rajendran, Sens. and Actuators B: Chemical, 147:290 (2010)

[31] T. Vijayalakshmi, R. Senthamarai, J. Supercomput. 78, 2477 (2022)

[32] G. Rahamathunissa, P. Manisankar, L. Rajendran, K. Venugopal, J. Math. Chem. 49, 457 (2011)

[33] R. U. Rani, L. Rajendran, M. E. Lyons, J. Electroanal. Chem. 886, 115103 (2021)

[34] S. Muthukaruppan, R. Senthamarai, L. Rajendran, Int. J. Electrochem. Sci. 7, 9122 (2012)

[35] K. Saranya, V. Mohan, L. Rajendran, J. Math. Chem. 58, 1230 (2020)

[36] K. Sankar Rao, Introduction to partial differential equations. PHI Learning Pvt. Ltd. (2010).